Journal of Petroleum Science and Engineering 215 (2022) 110642

Contents lists available at ScienceDirect

Journal of Petroleum Science and Engineering

journal homepage: www.elsevier.com/locate/petrol

Temperature-dependent rock physics modeling for heavy oil sands[1]

Junguang Nie [a,b], Xuehui Han [d], Jianhua Geng [a,b,c,*]

[a] State Key Laboratory of Marine Geology, Tongji University, China
[b] School of Ocean and Earth Science, Tongji University, China
[c] Center for Marine Resources, Tongji University, China
[d] China University of Petroleum (East China), China

ARTICLE INFO

Keywords:
Heavy oil sand
Heavy oil cementation
Temperature-dependent elastic property
Rock physics modeling

ABSTRACT

Heavy oil is considered an important alternative for traditional fossil fuels. Exploring and developing heavy oil reservoirs require time-lapse seismic data for dynamic monitoring of the reservoir elastic parameters and determining of the temperature field to evaluate the fluidity of the heavy oil. The key is establishing a relationship between the temperature and seismic elastic parameters to convert the elastic field into a temperature field. Therefore, a temperature-dependent rock physics model for heavy oil sand must be established. In this study, we investigated the temperature-dependent elastic wave velocities of natural and artificial heavy oil sands. The modified contact cement theory and the solid Gassmann equation were combined to construct a temperature-dependent rock physics model. The proposed model can predict variations in elastic wave velocities along with temperature changes in both natural and artificial heavy oil sands. Based on the model results, we propose a possible mechanism for the temperature-dependent elastic wave velocity of heavy oil sands, namely, the weakening of heavy oil cementation is the main controlling factor in the elastic wave velocity sensitivity of heavy oil sands. A temperature-dependent rock physics template (TDRPT) is proposed to diagnose the temperature, and the diagnostic results were verified using natural heavy oil sands. Our proposed model and TDRPT are essential tools to guide the thermal production of heavy oil reservoirs.

1. Introduction

Heavy oil reservoirs are essentially unconventional fossil fuel resources, and heavy oil reserves number almost three-fold those of conventional oil reservoirs worldwide (Meyer and Attanai, 2003). Further relevant exploration and development have facilitated the discovery of additional heavy oil reservoirs. However, heavy oil has high viscosity and cannot flow freely under in situ formation conditions; therefore, it is difficult to pump out.

Previous research has shown that temperature strongly affects the viscosity and elastic properties of heavy oil. An increase in temperature causes a rapid decrease in the viscosity and velocity of heavy oils (Wang and Nur, 1988; Han et al., 2006; Rojas et al., 2008; Yuan and Han, 2013; Yuan et al., 2016, 2018; Martinez et al., 2012; Li et al., 2016; Rabbni and Schmitt, 2018). Thermal recovery has been proven as the most efficient method for developing heavy oils. Therefore, dynamic monitoring of the temperature and physical differences in heavy oil reservoirs is necessary for thermal recovery (Zhao et al., 2017). For this purpose, geophysical methods, such as time-lapse seismic analysis, are applied conventionally (Schmitt, 1999; Nakayama et al., 2008). The rock physics model can build the relationship between seismic and heavy oil reservoir parameters. This model, therefore, is highly significant to establishing the temperature-velocity relations for heavy oil sands.

Temperature-dependent velocities of heavy oils have been investigated in laboratory studies (Han et al., 2006). Heavy oil can be divided into three stages according to its elastic response at different temperatures, namely, solid, quasi-solid, and liquid, as shown in Fig. 1. Glass point refers to the temperature at which the viscosity of heavy oil reaches 10^{12} Pas. Liquid point is the temperature corresponding to heavy oil viscosity of 1 Pas. Generally, heavy oil under formation conditions is mostly in the quasi-solid phase. Therefore, a primary method for developing heavy oil is to increase the temperature of the reservoir to reduce the viscosity, such that it can be converted from a quasi-solid to a liquid phase.

The temperature-dependent rock physics experiments for heavy oil sands have been reported in recent years. Yuan et al. (2016) investigated

[1] This research is financially supported by the National Natural Science Foundation of China (grant no. U20B6005).
* Corresponding author. State Key Laboratory of Marine Geology, Tongji University, China
E-mail address: jhgeng@tongji.edu.cn (J. Geng).

https://doi.org/10.1016/j.petrol.2022.110642
Received 21 October 2021; Received in revised form 10 April 2022; Accepted 12 May 2022
Available online 20 May 2022

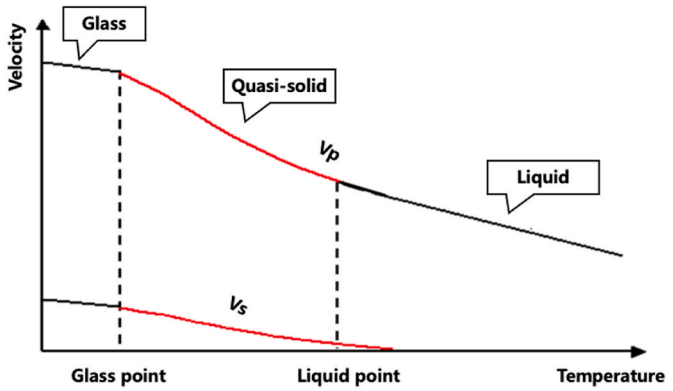

Fig. 1. Elastic velocities of heavy oil related to temperature in three phases (modified after Han et al., 2006). Here, V_p and V_s represent P- and S-wave velocities, respectively.

the temperature-dependent elastic properties of natural heavy oil sands in Alberta oilfield. Han et al. (2019) synthesized artificial heavy oil sands by controlling the ratio of heavy oil to quartz sand and measuring their elastic wave velocities at different temperature conditions. Yuan et al. (2020) experimentally investigate the temperature-dependent elastic properties of rock frame and two samples from Alaska and Alberta are compared, justifying the roles of bitumen and rock frame during the heating process. Li et al., 2022 measured elastic wave velocities for heavy oil sands samples under different saturations. Yuan et al. (2021) experimentally study the elastic wave velocities for North Sea heavy oil sands under changing pressure and temperature. These related experiments have important guiding significance for the mechanism and rock physics modeling of the temperature dependence of heavy oil sands.

Building a temperature-dependent rock physics model is complicated owing to the temperature-dependent elastic properties and phase changes of heavy oil during the heating process. However, various solutions have been proposed. For instance, Kato et al. (2008) proposed statistical rock physics models based on experimental data under different pressure and temperature conditions. Ciz and Shapiro (2007) extended the Gassmann equation (GE) for solid heavy oil saturation, and obtained a solid Gassmann equation (SGE) for rock physics modeling of heavy oil sands. Gurevich et al. (2008) employed the Cole–Cole and Maxwell models to study the frequency effects of heavy oil sands under different temperature conditions. To study the dispersion of heavy oil sands, Wang et al. (2017) modeled the viscoelastic properties of non-permeable porous rocks saturated with a highly viscous fluid at seismic frequencies and core scale. Wolf et al. (2006) established a rock physics model for heavy oil sands according to the heavy oil phases, with the heavy oil assumed to be cement in the pore space and the contact cement theory (CCT, Dvorkin et al., 1994) employed in the model. In the liquid phase, the GE is used to perform fluid substitution, whereas, in the quasi-solid phase, a temperature-related parameter is defined by arithmetically averaging the velocities of heavy oil sands between the solid and liquid phases of heavy oil (Dvorkin et al., 1994; Dvorkin and Nur, 1996; Gassmann, 1951). Yuan et al. (2016) introduced frame damage and solid oil proportion parameters to develop a new rock physics model. Zhang et al. (2018) employed the Xu–White model (Xu and White, 1995) to describe the temperature-dependent elastic wave velocities of heavy oil sands. Guo and Han (2016) considered the distribution of heavy oil in sand to establish rock physics models for heavy oil sands. However, all the studies mentioned neglected to investigate the effects of the temperature in heavy oil cementation on the temperature-dependent elastic properties. Accordingly, the focus of our study was building a temperature-dependent rock physics model that considers the cementation effect of heavy oil.

The paper is structured as follows. First, we introduce two sets of experimental data for natural and artificial heavy oil sands that include factors such as porosity, the relationship between temperature and the moduli of heavy oil, and that between temperature and the velocities of heavy oil sands, respectively. Second, we constructed a rock physics model based on the modified CCT and SGE. Third, we discuss the possible temperature-dependent mechanism of heavy oil sands and we estimate the temperature using a temperature-dependent rock physics model. Relevant conclusions bring the manuscript to a close.

2. Experimental data analysis

We used two experimental datasets from previous publications to study the temperature-dependent elastic wave velocities of heavy oil sands. One dataset pertains to natural heavy oil sands (Yuan et al., 2016) and the other to artificial heavy oil sands formed by mixing quartz sand and heavy oil (Han et al., 2019). The porosities of the samples are presented in Table 1. Additional experimental data and the details are available in the cited publications.

The porosities of the natural heavy oil sands are generally high, ranging from 34.88% to 44.24%, whereas those of artificial heavy oil sands are relatively low, ranging from 20.23% to 25.85%. These results are ascribed to the compaction pressure of the artificial samples (15 MPa) being higher than that of the natural samples (Yuan et al., 2016; Han et al., 2019).

2.1. Temperature-dependent elastic properties of heavy oil

The heavy oil of the natural samples derives from Alberta, Canada, whereas that of the artificial samples derives from the Shengli Oilfield, Eastern China. The American Petroleum Institute gravity (the API unit used to characterize the density of oil) indicates that the gravities of these oils differ, as well as their liquid points and temperature-dependent properties, as shown in Table 2.

The Rock Physics Laboratory of the University of Houston (USA) conducted numerous tests and gathered statistics on various fluids. Based on their experimental results, the Fluid of Applied Geophysics (FLAG) program was proposed to predict the elastic properties of fluids at different temperatures and pressures. We employed the FLAG program to predict the temperature-dependent bulk and shear moduli of the heavy oils from Alberta and Shengli. Negative linear relationships exist between the bulk modulus and temperature fitted by Equations (1) and (2), as shown in Fig. 2a.

$$K_{A\_ho} = -0.014T + 3.1242, \tag{1}$$

$$K_{S\_ho} = -0.0116T + 2.61, \tag{2}$$

where K_{A_ho} and K_{S_ho} represent the bulk moduli of the Alberta and Shengli heavy oils, respectively, and T represents the temperature.

Negative nonlinear relationships exist between the shear modulus and temperature, as shown in Fig. 2b. When the temperature is lower

Table 1
Porosity of natural and artificial heavy oil sands.

Sample No.	Type	Porosity (%)	Remarks
22#1	Natural sample	34.88	Pre-steam
22#2	Natural sample	43.17	Pre-steam
22#3	Natural sample	37.75	Pre-steam
23#1	Natural sample	41.06	Post-steam
23#2	Natural sample	44.24	Post-steam
23#3	Natural sample	40.77	Post-steam
9#1	Natural sample	41.25	Pre-steam
9#2	Natural sample	38.19	Pre-steam
APL-1	Artificial sample	25.85	Oil/sands mass ratio = 1:8
APL-2	Artificial sample	23.66	Oil/sands mass ratio = 1:9
APL-3	Artificial sample	21.81	Oil/sands mass ratio = 1:10
APL-4	Artificial sample	20.23	Oil/sands mass ratio = 1:11

Table 2
Liquid point, API gravity, and elastic modulus of heavy oil under different temperature conditions.

Source area	Properties					
	Liquid point (°C)	API gravity	Bulk modulus (GPa)		Shear modulus (GPa)	
			20 °C	100 °C	20 °C	100 °C
Heavy oil from Alberta (Canada)	57	7.5	2.8	1.7	0.1	0.0002
Heavy oil from Shengli (China)	43	15	2.4	1.5	0.02	0.0001

than the liquid point, the shear modulus decreases rapidly along with the increasing temperature. In comparison, when the temperature is higher than the liquid point, the shear modulus decreases to zero. The temperature-dependent shearing properties of the heavy oil of Alberta differ from those of Shengli because Alberta heavy oil has more light carbon components. The statistical relationships between the shear modulus and temperature are as follows:

$$G_{A\_ho} = 10317 * T^{-3.846}, \quad (3)$$

$$G_{S\_ho} = 157.9 * T^{-3.059}, \quad (4)$$

where G_{A_ho} and G_{S_ho} represent the shear moduli of the heavy oil from Alberta and Shengli, respectively.

2.2. Temperature-dependent elastic properties of heavy oil sands

The ultrasonic pulse transmission method was applied to measure the elastic velocities of natural and artificial heavy oil sands under different temperature conditions (Yuan et al., 2016; Han et al., 2019). Figs. 3 and 4 show the temperature-dependent P- and S-wave velocities of the natural and artificial heavy oil sands, respectively.

The velocities of both the natural and the artificial samples decrease along with an increase in temperature. The velocities of the artificial samples are significantly higher than those of the natural samples because of lower porosity caused by high compaction pressure. The results also indicate that the natural samples are more temperature dependent than the artificial samples, as shown by a comparison of their temperature change rates.

The velocity–temperature relationship of the artificial samples shows two apparent stages, namely when the temperature is lower than the liquid point, both P- and S-wave velocities decrease rapidly along with increasing temperature; however, when the temperature is higher than the liquid point, the velocity decreases only slightly. When the temperature is higher than the liquid point, the heavy oil changes from a quasi-solid state to the liquid stage (see Fig. 1), and the elastic properties of the heavy oil abruptly change, i.e., its shear modulus abruptly changes to zero. No obvious variations could be detected in the velocity change rate of some natural samples before and after the liquid point.

Furthermore, the relationships between the velocity, porosity, and mass fraction of the heavy oil are not monotonous in either the natural or the artificial heavy oil sands. The mass fraction of heavy oil (Vm) in the artificial heavy oil sands was in the following order: $Vm_{APL-1} > Vm_{APL-2} > Vm_{APL-3} > Vm_{APL-4}$, and the porosity showed the same behavior: $\varphi_{APL-1} > \varphi_{APL-2} > \varphi_{APL-3} > \varphi_{APL-4}$. However, the cor-

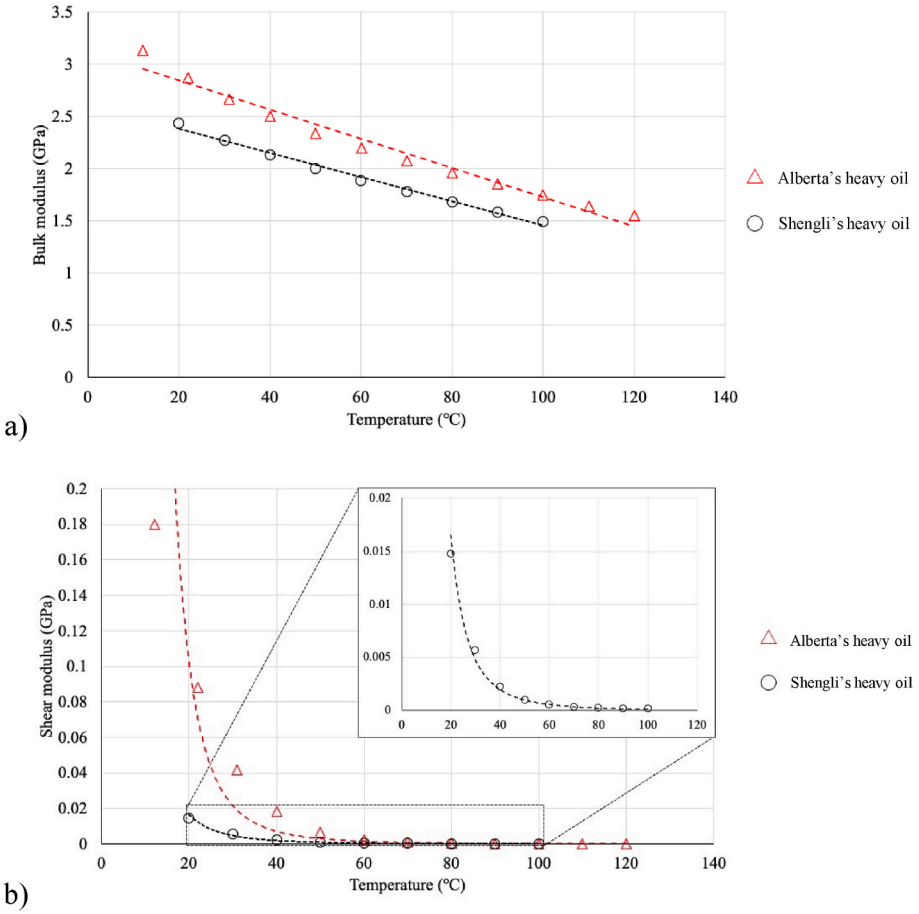

Fig. 2. Cross-plots of elastic modulus and temperature of heavy oil. (a) Bulk modulus and temperature; (b) shear modulus and temperature.

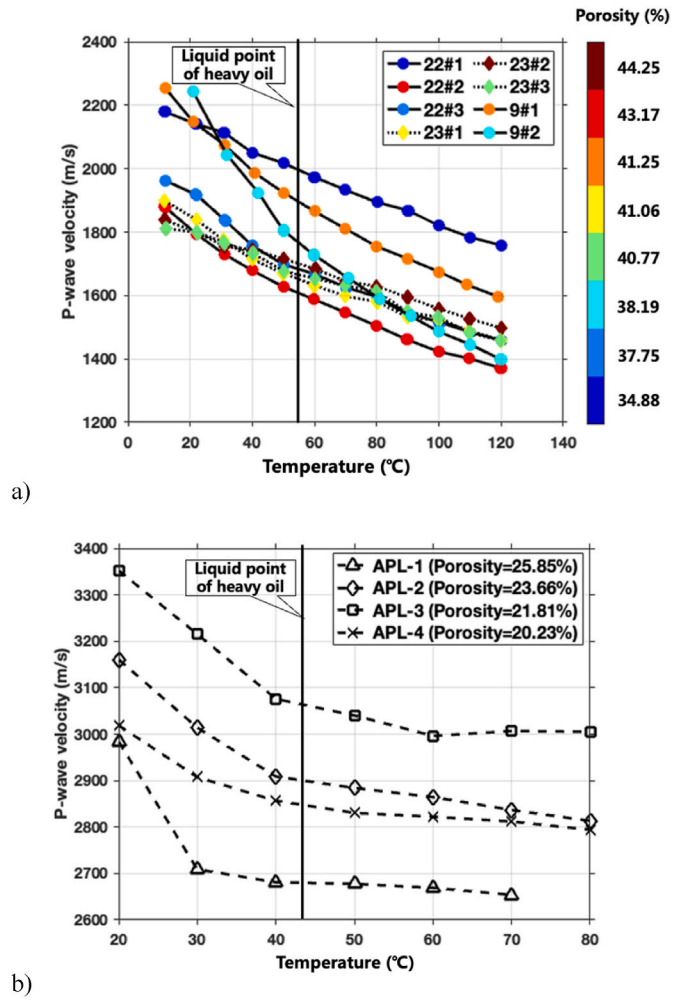

Fig. 3. Cross-plots of P-wave velocity and temperature. (a) Natural heavy oil sands of Alberta; (b) artificial heavy oil sands of Shengli. The black solid line indicates the liquid point.

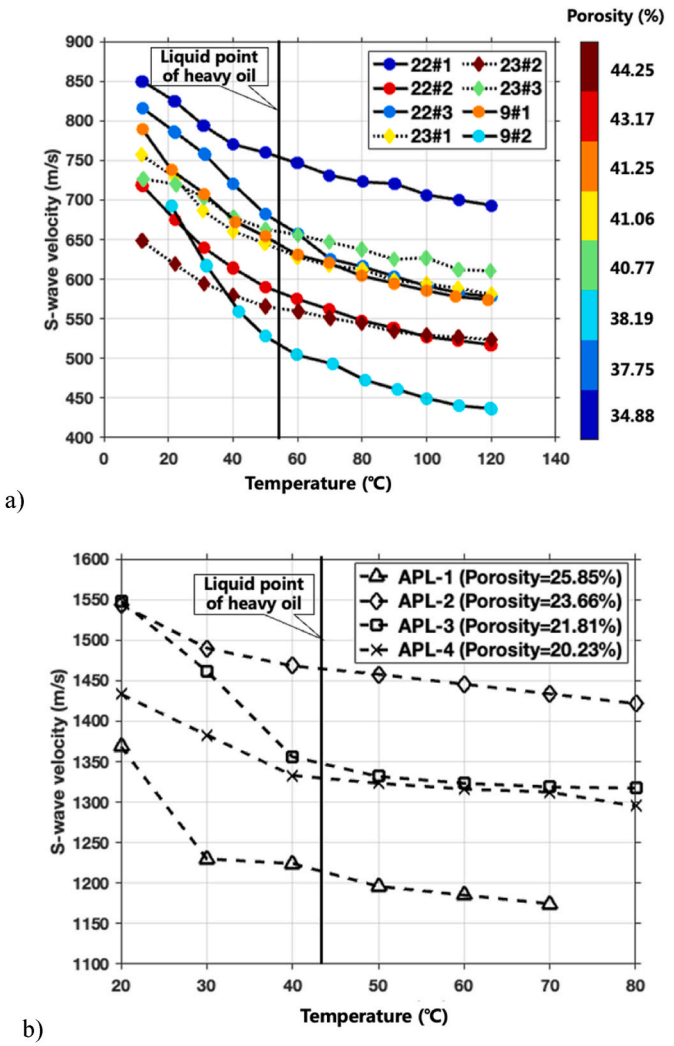

Fig. 4. Cross-plots of S-wave velocity and temperature. (a) Natural heavy oil sands of Alberta; (b) artificial heavy oil sands of Shengli. The black solid line indicates the liquid point.

responding P-wave velocity (*Vp*) and S-wave velocity (*Vs*) showed different changes in the order of $Vp_{APL-3} > Vp_{APL-2} > Vp_{APL-4} > Vp_{APL-1}$ and $Vs_{APL-2} > Vs_{APL-3} > Vs_{APL-4} > Vs_{APL-1}$. These phenomena indicated that in addition to porosity and the heavy oil content, other factors control the elastic wave velocity of heavy oil sands.

Previous study has shown that the rock skeleton of heavy oil sands is also temperature-dependent and it can be damaged during heating (Yuan et al., 2020). Heavy oil, as the cement in heavy oil sands, will affect elastic properties of rock skeleton. We speculate that the weakening of the cementation of heavy oil leads to the change of rock skeleton, because heavy oil sands' variation trends are similar to heavy oil's velocity-temperature trends (Fig. 1). Therefore, we will construct a rock physics model considering heavy oil cementation in the next section.

3. Rock physics modeling

Considering the cementation effect of heavy oil, we used the modified CCT in Equations (5) and (6) to calculate the temperature-dependent elastic modulus of the dry rock frame (Guo and Han, 2016).

$$K_{eff} = \frac{G_{ho(T)}(1-\nu_{ho(T)})}{1-2\nu_{ho(T)}} \frac{C(1-\varphi_o)}{3(1+\mathscr{E})} S_n, \tag{5}$$

$$G_{eff} = \frac{3}{5}K_{eff} + \frac{3G_{ho(T)}C(1-\varphi_o)}{20(1+\mathscr{E})} S_\tau, \tag{6}$$

where K_{eff} and G_{eff} are the bulk and shear moduli of the dry skeleton of the heavy oil sands, respectively; $G_{ho(T)}$ and $\nu_{ho(T)}$ are the temperature-dependent shear moduli and Poisson's ratio of the heavy oil, respectively; S_n and S_τ represent normal and tangential stiffness; φ_o is the original porosity; C is the coordination number; $\mathscr{E}$ is the contact thickness of the cement. The heavy oil content is related to the cementation radius, α, defined as (Mavko et al., 2009):

$$\alpha = a/R, \tag{7}$$

where a represents the radius of the heavy oil layer, R is the radius of the grain. When the heavy oil is distributed around the particles (called over-coating cement), which, in this study, is employed to describe the natural samples because of the high heavy oil content, the cementation radius (Mavko et al., 2009) α is

$$\alpha = \sqrt{\frac{2(\varphi_o - \varphi)}{3(1-\varphi_o)}}, \tag{8}$$

where φ represents porosity. When the heavy oil is distributed at the contact point of grains, called contact cement, which describes the artificial samples in this study because of the high compaction pressure and lower heavy oil content, the cementation radius α is

$$\alpha = \sqrt{-2\mathscr{E} + 2\sqrt{\mathscr{E}^2 + \frac{4}{3C}\frac{\varphi_o - \varphi}{1 - \varphi_o}}}. \tag{9}$$

The dry framework moduli of heavy oil sands can be calculated by combining Equations (5)–(9). We used solid Gassmann Equations (10) and (11) to calculate the elastic moduli of heavy oil saturated sands.

$$K_{sat} = K_{eff} + \frac{\left(1 - K_{eff}/K_{gr}\right)^2}{\frac{\varphi}{K_{fl}(T)} + \frac{1-\varphi}{K_{gr}} - \frac{K_{eff}}{K_{gr}^2}}, \tag{10}$$

$$G_{sat} = G_{eff} + \frac{\left(1 - G_{eff}/G_{gr}\right)^2}{\frac{\varphi}{G_{fl}(T)} + \frac{1-\varphi}{G_{gr}} - \frac{G_{eff}}{G_{gr}^2}}, \tag{11}$$

where K_{sat} and G_{sat} are the bulk and shear moduli of the heavy oil saturated sand, respectively; K_{eff} and G_{eff} are the bulk and shear moduli of the dry frame calculated with Equations (1) and (2), respectively; $K_{fl}(T)$ and $G_{fl}(T)$ are the temperature-dependent bulk and shear moduli of heavy oil; K_{gr} and G_{gr} are the bulk and shear moduli of the matrix grain, respectively. Then, the P- and S-wave velocities can be calculated using the following equations:

$$V_p = \sqrt{\frac{K_{eff} + \frac{4}{3}G_{eff}}{\rho_{eff}}}, \tag{12}$$

$$V_s = \sqrt{\frac{G_{eff}}{\rho_{eff}}}, \tag{13}$$

where V_p and V_s represent the P- and S-wave velocities of heavy oil saturated sands, respectively. ρ_{eff} represents the effective density of the heavy oil sands and is calculated using the following equation:

$$\rho_{eff} = (1 - \varphi)\rho_{gr} + \varphi\rho_{ho}, \tag{14}$$

where ρ_{gr} and ρ_{ho} represent the densities of the matrix grains and heavy oil, respectively. The temperature-dependent elastic wave velocities of the heavy oil sands can be calculated by combining Equations (5)–(14). The input parameters are listed in Table 3.

For comparison, we combined the Hertz–Mindlin model with the Hashin–Shtrikman lower bound (HMHS model, Dvorkin and Nur, 1996) and the SGE to model the elastic wave velocity of the natural heavy oil sands samples (Yuan et al., 2016). We chose sample 22#1 as a reference to analyze the modeled results, as shown in Fig. 5.

The comparison indicates that the P- and S-wave velocities calculated by HMHS are significantly higher than the experimental results, in particular the S-wave velocities, whereas the velocities calculated by the modified CCT are close to the experimental results. This finding reasonably indicates the temperature-dependent elastic properties of the natural samples. The HMHS model is known as an unconsolidated sandstone model (noncement model). The reason for the lower prediction results of the modified CCT compared with those of the unconsolidated sandstone model is probably overestimation by the unconsolidated sandstone model of the contact stiffness of the rock, as this model assumes that the particles are in direct contact. In natural heavy oil reservoirs, particles are more likely to be in contact with heavy oil than in direct contact (Yuan et al., 2016). However, the proposed model does not accurately match the test results. When heavy oil cementation is weakened, the properties of the skeleton could change nonlinearly. Microscopic behaviors, such as translation and rotation of sand particles are complex and random and challenging for models to characterize; therefore, perfect matching is difficult.

We used the same modeling technique of modified CCT to predict the elastic wave velocities of artificial sample APL-1, as shown in Fig. 6. The model input parameters are listed in Table 3. The predicted elastic wave velocity shows a temperature-related trend. The relative errors are shown in Fig. 7 for both the natural and the artificial samples are less than 10%, and the predicted errors are temperature dependent. Accordingly, the parameters in the modified CCT, such as cementation thickness, should also be temperature dependent. We noticed a non-monotonic change in the error–temperature relation of sample APL-1. The rock physics model assumes stable contact between skeleton

Table 3
Parameters for modeling natural and artificial samples.

Parameters	Values
Bulk modulus of matrix grain: K_{gr}	37 GPa
Shear modulus of matrix grain: G_{gr}	44 GPa
Density of matrix grain: ρ_{gr}	2.65 g/cm^3
Parameters for natural sample 22#1	
Original porosity: φ_{on}	0.4 (volume fraction)
Porosity:φ_n	0.35 (volume fraction)
Cementation thickness: $\mathscr{E}$	0.052 (dimensionless)
Coordination number: C_n	7.5 (dimensionless)
Parameters for artificial sample APL-1	
Original porosity: φ_{oa}	0.36 (volume fraction)
Porosity: φ_a	0.26 (volume fraction)
Cementation thickness: $\mathscr{E}$	0 (dimensionless)
Coordination number: C_a	9 (dimensionless)

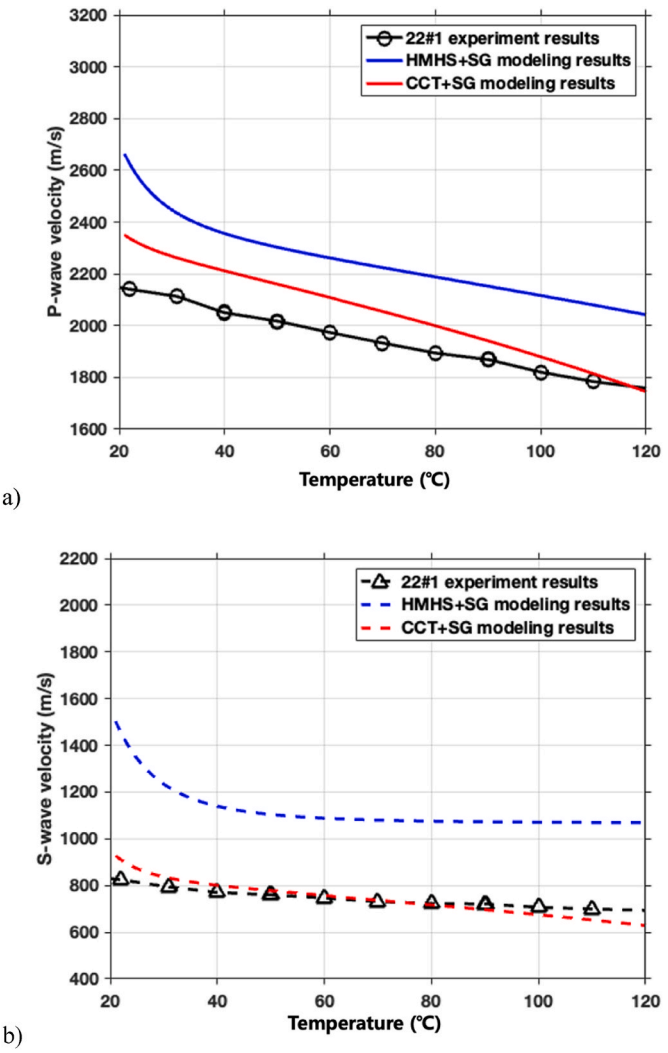

Fig. 5. Modeling and experimental P- (a) and S-wave (b) velocities of sample 22#1. The black dashed line with triangles, and the red and blue dashed lines represent the experimental data modeled by the modified CCT and HMHS, respectively.

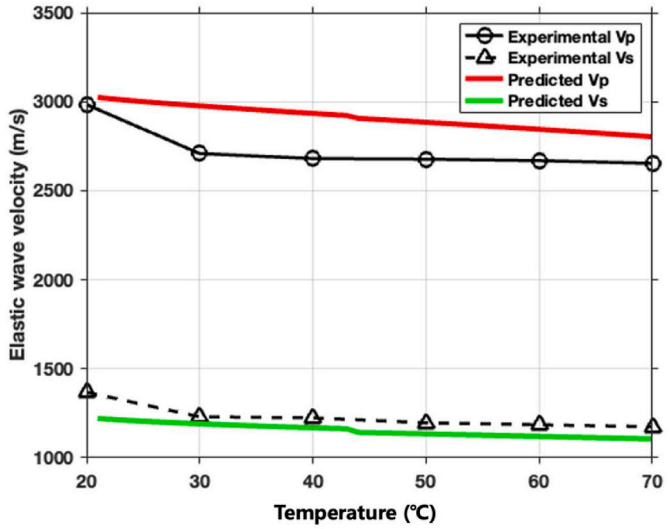

Fig. 6. Modeling results for artificial sample APL-1. (a) The black solid and the dashed lines represent experimental P- and S-wave velocities, respectively. The solid red and green lines represent the predicted P- and S-wave velocities, respectively.

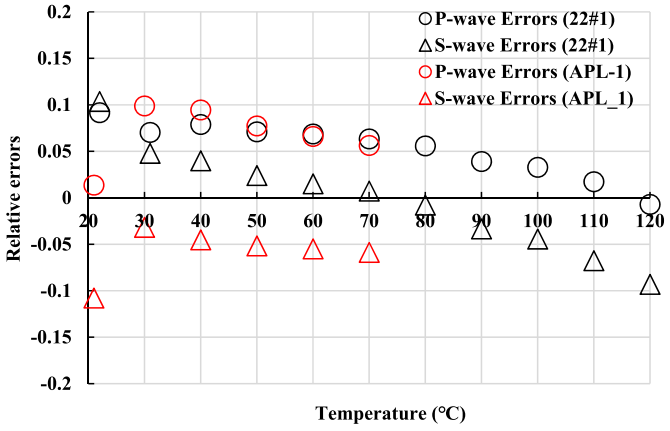

Fig. 7. Cross-plot of relative errors and temperature.

particles. However, heavy oil cementation gradually weakens along with an increase in temperature, which could lead to unstable contact between the particles and could cause sudden changes in elastic velocities. This model cannot be employed to simulate mutations in elastic wave velocity.

4. Discussion

4.1. Temperature-dependent mechanism of elastic properties of heavy oil sands

Previous rock physics models do not consider cementation effects, but treat heavy oil as filling pores or being part of the rock frame to explain the mechanism of temperature-dependent elastic wave velocities. In this study, we treated heavy oil as cement in heavy oil sands and we used the modified cemented theory to simulate the temperature-dependent elastic wave velocities of both artificial and natural heavy oil sands. We found that the weakening of cementation could be a possible mechanism for the temperature-dependent elastic properties of heavy oil sands.

However, such interpretation requires more evidence, such as variations in the microstructure of heavy oil sands with increasing temperature. In future research, we suggest developing experimental technologies for dynamic computed tomography scan imaging to examine changes in the contact between the particles and heavy oil during a temperature rise.

4.2. Diagnosing the temperature of heavy oil sands

Based on the modified rock physics model, we constructed a temperature-dependent rock physics template (TDRPT), a cross-plot of Poisson's ratio and P-wave impedance, to estimate the temperature stage of heavy oil sands. Details on the workflow follow.

1) Use the FLAG program to calculate the temperature-dependent elastic modulus of the heavy oil.
2) Use the core data to determine parameters in the temperature-dependent rock physics model.
3) Investigate the influence of different cementation thicknesses and temperatures on Poisson's ratio and P-wave impedance based on rock physics modeling.
4) Superimpose the actual and modeled data on the TDRPT and reasonably adjust the input parameters, such as the coordination number and original porosity, to keep the TDRPT consistent with the actual data.
5) Estimate the temperature of heavy oil sands according to the TDRPT.

Based on the above workflow, we used the rock physics parameters of sample 22#1 to establish a TDRPT, as shown in Fig. 8. The P-wave impedance decreases with an increase in cementation thickness and temperature. If the temperature is lower than the liquid point, Poisson's ratio rapidly increases along with the increasing temperature. If the temperature is higher than the liquid point, when the cementation thickness is 0, Poisson's ratio slowly decreases as the temperature rises. When the cementation thickness is 0.0625, Poisson's ratio slowly increases as the temperature rises, and when the cementation thickness is between 0.015 and 0.05, Poisson's ratio remains nearly unchanged as the temperature rises. Therefore, Poisson's ratio is influenced by the joint effect of temperature and cementation thickness. The diamond dots on TDRPT in Fig. 8 show the temperature-dependent elastic properties of sample 22#1. When the temperature is higher than 90 °C, the TDRPT measures the temperature of the sample extremely well. When the temperature is below 90 °C, although errors occur in estimating the sample temperature, the TDRPT still depicts the trend in temperature

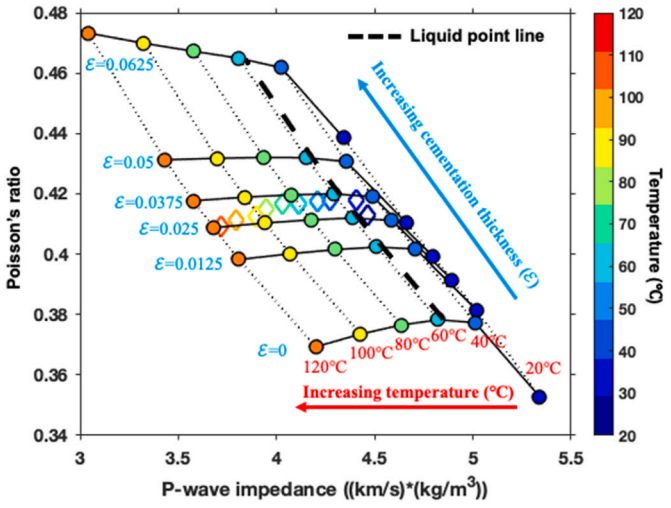

Fig. 8. TDRPT for sample 22#1. The diamond dots represent the experimental data, and the circle dots represent the modeling results. The black dashed line represents the liquid point line. The blue and red numbers represent the cementation thickness and temperature, respectively.

change in sample 22#1. Accordingly, considering the elastic properties of subsurface heavy oil reservoirs inverted from seismic reflection data on the TDRPT, the heavy oil reservoir temperature can be estimated by using surface seismic data. However, accurate estimation of the subsurface temperature by TDRPT remains challenging owing to the influence of several other factors, such as the shale content, mineral types, and coordination number.

The proposed TDRPT could guide the dynamic detection of heavy oil reservoirs, evaluate the heating range of heavy oil, and evaluate the recoverability of the heavy oil. Moreover, the proposed TDRPT lays the foundation for quantitative seismic evaluation of heavy oil sand reservoirs. The elastic modulus–temperature relationship of the heavy oil should be obtained before employing TDRPT. Subsequently, the basic geological background of the target zone should be determined, such as the lithology of the framework, range of porosity, and compaction degree (coordination number). Such information could be obtained from the well-logging data of drilling records. Compared with traditional experimental empirical relationships, the TDRPT we developed is quantitative, generalizable, and easy to use.

Further, the elastic wave velocities of both the natural and the artificial samples were measured during this study using ultrasonic waves with a frequency of 10^5–10^6 Hz (Yuan et al., 2019; Han et al., 2019), whereas the frequency of the seismic elastic properties ranged from 10^0 to 10^2 Hz. Previous studies (Schmitt, 1999; Gurevich et al., 2008) have indicated that heavy oil sands at low frequencies (10^0–10^2 Hz) show higher temperature sensitivity compared with those at high frequencies (10^4–10^6 Hz). Therefore, when processing seismic data, it is necessary to modify the proposed TDRPT for low-frequency seismic waves. The effect of temperature on the cementation of heavy oil under low-frequency conditions remains unclear. Studies on both frequency-variant and temperature-dependent rock physics modeling for heavy oil sands are challenges that need to be resolved in the future.

5. Conclusion

In this study, we used natural and artificial heavy oil sands as examples to study their temperature-dependent elastic wave velocities. The experimental data showed that the elastic wave velocities of both natural and artificial heavy oil sands decreased with increasing temperature. Both types of samples showed different temperature sensitivities, ascribed to the different types of heavy oils. The elastic wave velocities of the artificial samples were systematically higher than those of the natural samples because of higher compaction pressure.

We proposed a temperature-dependent rock physics model for heavy oil sands based on the modified CCT and SGE. The proposed model was verified by both natural and artificial heavy oil sands, and the predicted errors of the P-wave and S-wave velocities were lower than 10%. We proposed a possible mechanism for the temperature-dependent elastic properties of heavy oil sands, namely, the temperature-dependent elastic properties of heavy oil sands could be caused by the weakening of heavy oil cementation with an increasing temperature. Based on our proposed model, we presented a TDRPT to diagnose the temperature, which we verified using the natural heavy oil sand samples. The proposed temperature-dependent rock physics model and TDRPT provide significant guidance for the development and evaluation of heavy oil thermal production.

Credit author statement

Junguang Nie: Conceptualization; Methodology; Software; Investigation; Writing – original draft. **Xuehui Han**: Resources; Data curation. **Jianhua Geng**: Conceptualization; Validation; Resources; Writing – review & editing; Supervision; Project administration.

Data availability

Data sharing is not applicable to this article as no new data were created in this study. The data used in this paper are those described in the articles by Han et al. (2019) and Yuan et al. (2016) cited in this paper.

Declaration of competing interest

The authors declare that they have no known competing financial interests or personal relationships that could have appeared to influence the work reported in this paper.

References

Ciz, R., Shapiro, S.A., 2007. Generalization of Gassmann equation for porous media saturated with a solid material. Geophysics 72 (6), A75–A790.
Dvorkin, J., Nur, A., 1996. Elasticity of high-porosity sandstones: theory for two North Sea data sets. Geophysics 61 (5), 1363–1370.
Dvorkin, J., Nur, A., Yin, H., 1994. Effective properties of cemented granular materials. Mech. Mater. 18 (4), 351–366.
Gassmann, F., 1951. Über die Elastizität poroser medien :Veirteljahrsschrift der Naturforschenden. Gesellschaft in Zürich, pp. 1–23.
Guo, J., Han, X., 2016. Rock physics modelling of acoustic velocities for heavy oil sand. J. Petrol. Sci. Eng. 145, 436–443.
Gurevich, B., Osypov, K., Ciz, R., Makarynska, D., 2008. Modeling elastic wave velocities and attenuation in rocks saturated with heavy oil. Geophysics 73 (4), D453–D464.
Han, D., Liu, J., Batzle, M., 2006. Acoustic Property of Heavy Oil Measured Data. SEG Technical Program Expanded Abstracts, pp. 1903–1907.
Han, X., Li, H., Nie, J., Shen, G., Jiang, J., Li, J., 2019. The acoustic velocity of artificial heavy oil sands and rock physics modelling. In: EAGE Conference and Exhibition.
Kato, A., Onozuka, S., Nakayama, T., 2008. Elastic property changes in a bitumen reservoir during steam injection. Lead. Edge 27 (9), 114–1131.
Li, H., Han, D., Sun, M., Yuan, H., Gao, J., 2022. An experimental investigation on effects of saturation levels and fluid types on elastic properties of bitumen-saturated sands at elevated temperatures. Energy 238, 122011.
Li, H., Zhao, L., Han, D., Sun, M., Zhang, Y., 2016. Elastic properties of heavy oil sands: effects of temperature, pressure, and microstructure. Geophysics 81 (4), D453–D464.
Martinez, F.J., Batzle, M.L., Revil, A., 2012. Influence of temperature on seismic velocities and complex conductivity of heavy oil-bearing sands. Geophysics 77, WA19–WA34.
Mavko, G., Mukerji, T., Dvorkin, J., 2009. The Rock Physics Handbook: Tools for Seismic Analysis in Porous Media. Cambridge University Press.
Meyer, R., Attanai, E.D., 2003. Heavy oil and natural bitumen: strategic petroleum resources. US Geol. Surv.
Nakayama, T., Takahashi, A., Skinner, L., Kato, A., 2008. Oil sands reservoir monitoring using time-lapse 3D seismic in Canada. In: International Petroleum Technology Conference.
Rabbni, A., Schmitt, D.R., 2018. Ultrasonic shear wave reflectometry applied to the determination of the shear moduli and viscosity of a viscoelastic bitumen. Fuel 232 (15), 506–528.
Rojas, M.A., Castagna, J., Krishnamoorti, R., Han, D., Tutuncu, A., 2008. Shear thinning behavior of heavy oil samples: laboratory measurements and modeling. SEG Tech. Progr. Expand. Abstr. 27 (1), 1710–1714.
Schmitt, D.R., 1999. Seismic attributes for monitoring of a shallow heated heavy oil reservoir: a case study. Geophysics 64 (2), 368–377.
Wang, Z., Schmitt, D.R., Wang, R., 2017. Modeling of viscoelastic properties of nonpermeable porous rocks saturated with highly viscous fluid at seismic frequencies at the core scale. J. Geophys. Res. Solid Earth 122 (8).
Wang, Z., Nur, A., 1988. Effect of temperature on wave velocities in sands and sandstones with heavy hydrocarbons. SPE Reservoir Eng. 3 (1), 158–164.
Wolf, K., Mukerji, T., Mavko, G., 2006. Attenuation and Velocity Dispersion Modeling of Bitumen Saturated Sand. SEG Technical Program Expanded Abstracts, pp. 1993–1997.
Xu, S., White, R.E., 1995. A new velocity model for clay-sand mixtures. Geophys. Prospect. 43 (1), 91–118.
Yuan, H., Han, D., 2013. Pressure and Temperature Effect on Heavy Oil Sand Properties. SEG Technical Program, pp. 2984–2988.
Yuan, H., Han, D., Huang, Q., 2018. Laboratory Studies of Artificial Oil Sands Samples. EAGE Conference and Exhibition.
Yuan, H., Han, D., Zhang, W., 2016. Heavy oil sands measurement and rock-physics modelling. Geophysics 81 (1), D57–D70.
Yuan, H., Han, D., Li, H., Zhao, L., Zhang, W., 2020. The effect of rock frame on elastic properties of bitumen sands. J. Petrol. Sci. Eng. 164, 107460.
Yuan, H., Han, D., Zhao, L., Qi, H., Zhang, W., 2019. Attenuation analysis of heavy oil sands based on laboratory measurements. Geophysics 84 (5), B299.

Yuan, H., Wang, Y., Han, D., Li, H., Zhao, L., 2021. Velocity measurement of North Sea heavy oil sands under changing pressure and temperature. J. Petrol. Sci. Eng. 205, 108825.

Zhang, J., Li, H., Yin, X., Zhang, G., Lv, C., Fan, X., 2018. A rock physics model for heavy oil sandstones by combing Xu-White model and generalized Gassmann equations. In: EAGE Conference and Exhibition.

Zhao, L., Yuan, H., Yang, J., Han, D., Geng, J., Zhou, R., et al., 2017. Mobility effect on poroelastic seismic signatures in partially saturated rocks with applications in time-lapse monitoring of a heavy oil reservoir. J. Geophys. Res. Solid Earth 122 (11), 8872–8891.